Crimson Publishers
Wings to the Research

Research Article

Visible Light Photocatalytic-Adsorption Effect of Recyclable Industrial Waste

ISSN: 2578-0255

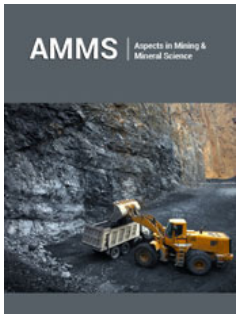

***Corresponding author:** Katalin Sinkó, Institute of Chemistry, Eötvös Lóránd University, H-1117, Budapest, Hungary

Submission: March 07, 2025
Published: March 19, 2025

Volume 13 - Issue 2

How to cite this article: János Kóth and Katalin Sinkó*. Visible Light Photocatalytic-Adsorption Effect of Recyclable Industrial Waste. Aspects Min Miner Sci. 13(2). AMMS. 000808. 2025.
DOI: 10.31031/AMMS.2025.13.000808

János Kóth and Katalin Sinkó*

Institute of Chemistry, Eötvös Lóránd University, Hungary

Abstract

Removal of the contaminants/organic dye pollutants from wastewater provides a relevant global challenge. In this work the photodegradation of organic pollutants was aimed to realise by means of a very dangerous, toxic industrial waste, the red mud. Beside of the environmental aspect, the economic respect was also considered by recycling of an industrial waste and using visible region for photodegradation instead of generally applied ultraviolet light. The photocatalytic properties of Red Mud (RM) were tested in the solution of analytical indicators used as model agents (methylene blue, Congo red, and crystal violet) and real organic pollutants (cortisone and corticosterone). The mechanism of degradation effect (photocatalytic effect and/or adsorption) has been clarified. The degradation effect of RM was detected using Ultraviolet-Visible (UV-VIS) and fluorescence spectroscopies. The connections between pollutants and red mud were investigated by infrared spectroscopy (FTIR)

Keywords: Red mud; Recycling; Wastewater; Photocatalysis; Adsorption

Introduction

One of the important goals of environmental protection is to recycle the huge amount of industrial waste and the other is to get clear water. Red mud (RM) industrial waste has been produced during alumina production, generating around 175 million tons of RM as a by-product [1]. The utilization rate of RM is only about 1-2% [2], The red mud can be characterised by high alkalinity, toxicity, and radioactivity [3]. RM is a fine-grained, red-coloured mixture of oxides (Fe_2O_3, Al_2O_3, TiO_2, SiO_2, CaO, Na_2O, etc.) [4]. Currently, the majority of RM is disposed in landfills [5,6]. Its other notable application can be observed in the field of building materials [7-9], however, only in a few countries. It can be used as a component of ceramic products [10], retarders [11], pH buffers [12] and heavy metal ion removal [13]. The contaminants of water, often considered emerging pollutants, pose a severe risk to the quality of fresh water, human health, and ecosystems. The deliberate discharge of dyes and antibiotic wastewater becomes a serious threat to human society [14-16] Various techniques have been developed to treat such pharmaceutical wastewater, including membrane techniques, biological treatment, physisorption, and photocatalytic degradation [17-20]. Among these, adsorption and photocatalytic degradation are particularly effective and economical methods for removing organic contaminants from water [21-23]. However, the separate use of each method has limitations, such as adsorption capacity and photocatalytic efficiency. The persistent challenge of reducing these contaminants, such as Pharmaceutically Active Compounds (PACs), necessitates the development of innovative materials and techniques with enhanced adsorption and photocatalytic activity [24,25].

Certain components of red mud have been published with adsorption or/and photocatalytic effects. Titanium-dioxide (TiO_2) are commonly used as photocatalytic materials for wastewater purification [26-28]. However, TiO_2 is well known about excellent photocatalytic effect but its use is expensive due to required ultraviolet region and the high price of TiO_2 [29]. Hematite has also been studied for the photocatalytic degradation of organic contaminants [30]. Weak photocatalytic effect is published for pure hematite. Hematite due to the narrow band gap of 2.0-2.2eV, can be efficient in visible light up to 600nm [31]. Other noteworthy characteristics, such as excellent stability, low toxicity, cost-effectiveness, inert behaviour, and antiferromagnetic properties, contribute to its broad range of applications [32-34]. There is published data about methylene blue degradation by effect of red mud containing systems but the compositions of these systems are different from our samples [35-37]. The aim of present study was the recycling of the industrial waste, such as very dangerous, toxic red mud as a waste of aluminium industrial fabrication. In this work a new special application of red mud has been developed regarding the environmental aspect. That is the reduction of organic water pollution by RD in visible light. By this way two environmentally friendly aims can be achieved; the reprocessing of a toxic waste material and cleaning the waters.

The investigation of photoactive properties of RM was performed in the solution of analytical indicators used as model agents (methylene blue, Congo red and crystal violet indicators). The mechanism of degradation effect (photodegradation and/or adsorption) has been clarified. Real organic "waste" components were also tested by red mud application. The degradation effect of RM was determined using Ultraviolet-Visible (UV-VIS) and fluorescence spectroscopies. The connections between pollutants and red mud were investigated by infrared spectroscopy (FTIR). The characterisation of red mud was carried out by thermal analysis and X-ray diffraction techniques.

Experiments

Preparation methods

Between from the various materials used in the water cleaning, the red mud was washed with distilled water until to get 7 pH and dried at 100 °C, then milled to reach the particle diameters of 200-400µm. Aqueous solutions of analytical indicators (methylene blue, Congo red, and crystal violet) were used with concentration of 1.2–5.0 10-4mol/dm3. 5 grams of red mud powder was added to 50cm^3 solutions. The time of the treatment with visible light was varied between 1 and 8 hours. The other materials, such as organic pollutants (cortisone and corticosterone) were used in aqueous or alcoholic solutions with 7.5·10-3 mol/dm^3 concentration. Instead of red mud, its synthetic compounds and the mixture of synthetic compounds were tested as well as chitosan was applied for comparison.

Investigation methods

Powder X-Ray Diffraction measurements (XRD) were performed by a Rigaku Smartlab X-ray diffractometer equipped with a 1.2kW copper source (radiation wavelength: CuKα; λ=0.15418nm). The data were collected in the range 2Θ between 10° and 110° with a 1D silicon strip detector (D/Tex ultra-250) at a speed of 0.2°/min. The results were analysed using databases, such as ICDD, and other data from the literature. Thermal analysis measurements were conducted using Derivatograph-C System equipment between 25 °C and 1000 °C, under static air atmosphere, with 10 °C/minute heating rate. The weight change of the samples was followed with respect to the temperature by Thermogravimetry (TG), the exothermic and endothermic changes were detected by Differential Thermal Analysis (DTA). The sample holder's material and the reference material were aluminium oxide.

Attenuated Total Reflectance (ATR) Fourier Transform Infrared (FTIR) measurements were recorded on a Bruker IFS 55 instrument with a diamond ATR head (PIKE Technologies). The transmission mid-IR spectra were taken during and after the deposition by averaging 128 scans, respectively, in the 4000-600cm−1 region with 1cm−1 resolution using MTR detector cooled with liquid nitrogen, and KBr splitter. Photodegradation measurements was realised by using a LED light, model number: Eulbevoli68r34z052u408. with the following parameters: 50W power, 4500-5000lm luminous flux and 380-840nm wavelength from a 15cm distance. Fluorescence spectroscopy measurements were recorded using a Varian Cary Eclipse spectrofluorometer (Agilent Technologies, Santa Clara, CA, USA). The following settings were used: excitation: λ=360nm; emission: λ=190-500nm; detector voltage: 450V. Ultraviolet and visible light (UV-VIS) spectroscopy measurements were realised using a Thermo Spectronic Helios Gamma instrument.

Result and Discussion

Characterisation of red mud

Red Mud (RM) was characterised by XRD (Figure 1) and thermal analysis (Figure 2). The main components of original RM used in this study are hematite (α-Fe_2O_3) and cancrinite ($Na_6Ca_2[(CO_3)_2|Al_6Si_6O_{24}]\cdot 2H_2O$); RM contains even calcite ($CaCO_3$), Ca titanate (CaTiO3), and goethite (FeO(OH)) in smaller amounts; crystalline phase of rutile (TiO_2), boehmite (AlO(OH)), and gibbsite ($Al(OH)_3$) can be detected only in very low volume by XRD. Detectable changes cannot be observed by washing in the crystalline phases (Figure 1). Mostly aqueous NaOH content is removed by washing step. The reduction of amount was 36-39% during the washing. The drying process up to 500 °C resulted in further 7-8% reduction in the volume; boehmite, gibbsite, goethite, and rutile crystalline phases disappeared. The most relevant chemical compounds of original RM are represented in oxide form: 32-38% Fe_2O_3, 16-18% Al_2O_3, 8-12% SiO_2, 7-10% Na_2O, 4-5% TiO_2, 1-3% CaO (XRF measurements).

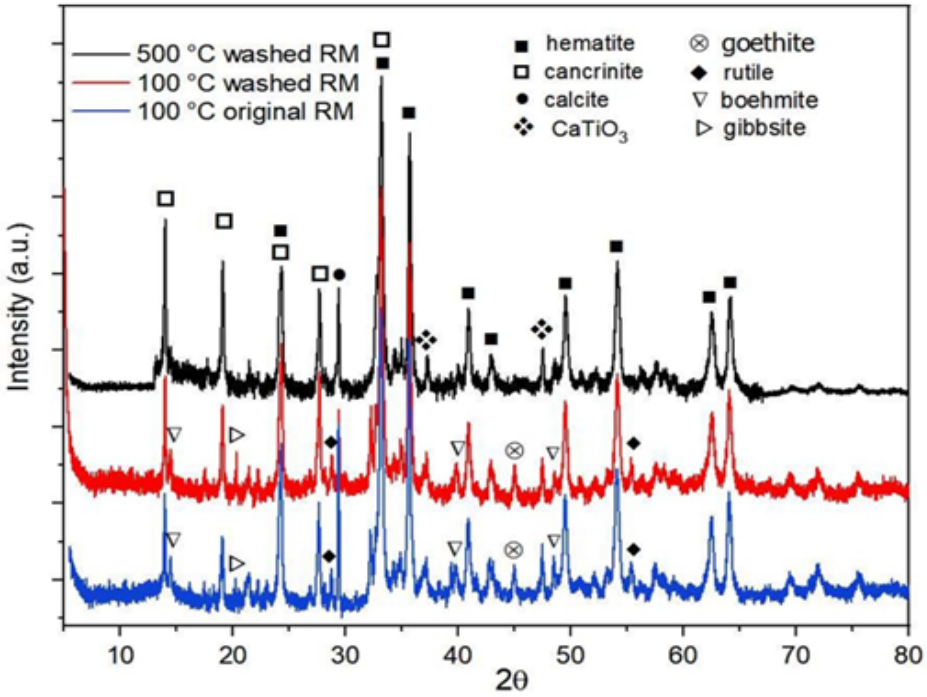

Figure 1: Phase composition of red mud vs. temperature. XRD measurements.

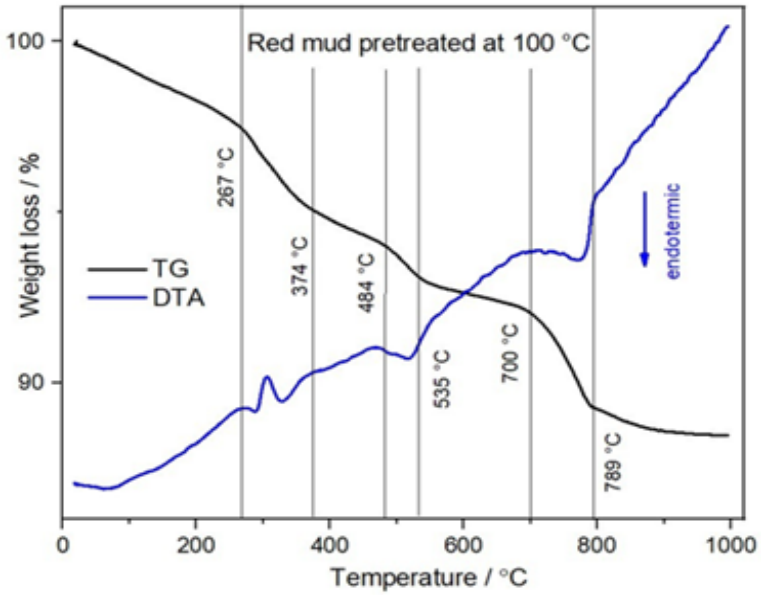

Figure 2: Thermal analysis of red med pretreated at 100 °C.

The changes of red mud phases during the heating have been determined by Thermal Analysis (TA) (Figure 2). The weight loss of the original red mud was 30-31% until 100 °C without washing. In order to represent the TA data well observably, RM was dried at 100 °C and it was used in TA measurements. The total weight loss was 11-12% above 100 °C. The weight loss between 267 and 374 °C is derived from the loose of water from various phases (gibbsite, boehmite, and cancrinite) [38,39]. At around 360 °C the decomposition of goethite occurs to hematite. In the range of 484-535 °C, the endothermic peak and weight loss connects to the transformation of boehmite to transition γ-Al2O3 phase [38,39]. The weight loss and endothermic peak in the range of 700-800 °C can be derived from decomposition of calcite. The other reactions of the released CaO must be calculated above 700 °C; $2CaO+SiO_2 \rightarrow Ca_2SiO_4$ and $Ca_2SiO_4+SiO_2 \rightarrow 2CaSiO_3$ [40].

Photodegradation-adsorption effect of red mud

The first tests for degradation ability of RD were performed with analytical indicators as model agents (methylene blue, Congo red, and crystal violet). The results of two types, i.e. Methylene Blue

(MB) and Crystal Violet (CV) are presented in Figure 3. The reduction of MB was 79,3 % after 4 hours' treatment by visible light, and in the case of CV was 77,6%. Congo red model agent was degraded by >90% after 1 hour. For further investigation Methylene Blue (MB) was selected owing to its better control. In order to decide that the adsorption must be taken into account or only photocatalytic effect, tests were performed with and without light (in dark). The result of MB has proved the considerable adsorption ability of red mud (Figure 4). After 2 hours' treatment of a solution in visible light and another solution in dark, the concentration of MB was reduced by 95.0% and 84.6%, respectively. That means 89% adsorption and 11% photocatalytic effect in the case of methylene blue. FTIR spectroscopy checked the interaction between the MB and red mud (Figure 5). FTIR does not reveal a regular connection but presents a broad deviation between 3350 and 3650cm^{-1} denotes a loose interaction between MB and RM confirming the adsorption.

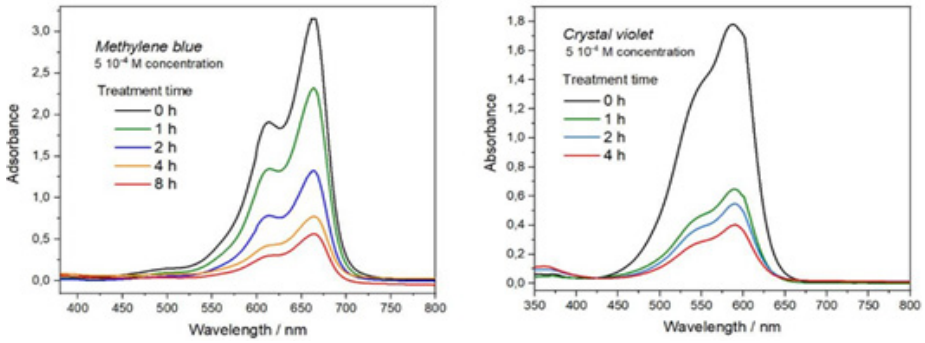

Figure 3: Photodegradation-adsorption of model agents by red mud in visible light region from aqueous solution. UV-VIS absorption measurements.

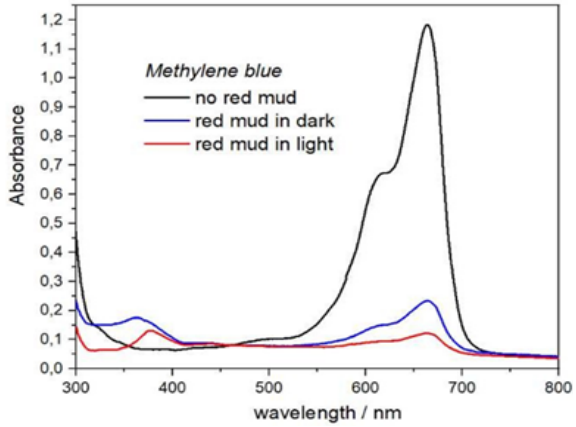

Figure 4: Investigation of photodegradation and adsorption effects of red mud in visible light region and without lighting in 1.25 10^{-4}mol/dm^3 aqueous solution of model agent. UV-VIS absorption measurements.

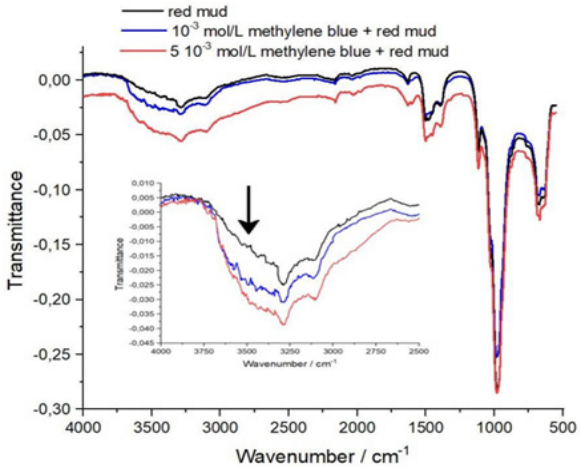

Figure 5: Infrared spectra of red mud-methylene blue systems after visible light treatment.

In order to determine the role of components in the degradation effect, the influence of hematite content was studied at first (Figure 6 & Table 1). Hematite represents the largest component in RM, 32-38%. The various amount of hematite was mixture with Al_2O_3. In summary, the higher the hematite fraction the lower the reduction effect is. It means Al_2O_3 has an important role especially in the adsorption. It is well known that Al_2O_3 possesses good adsorption ability. The best reduction can be achieved with use of 100% Al2O3 (68.5%) but this value is still much lower than the pure red mud produces, 80.1% (Table 1). The investigation of the degradation of MB in the function of hematite - aluminium oxide mixtures did not result in a completely adequate interpretation for the degradation effect of red mud' components. Thus, the Fe_2O_3 and Al2O3 components were extended by further components (Figure 7). The pure aluminium oxide proved to be again the most efficient compound, after that hematite. The synthetic rutile and calcite only decrease the efficiency. Therefore, the smaller components of red mud and their morphology have important role in the photodegradation effect.

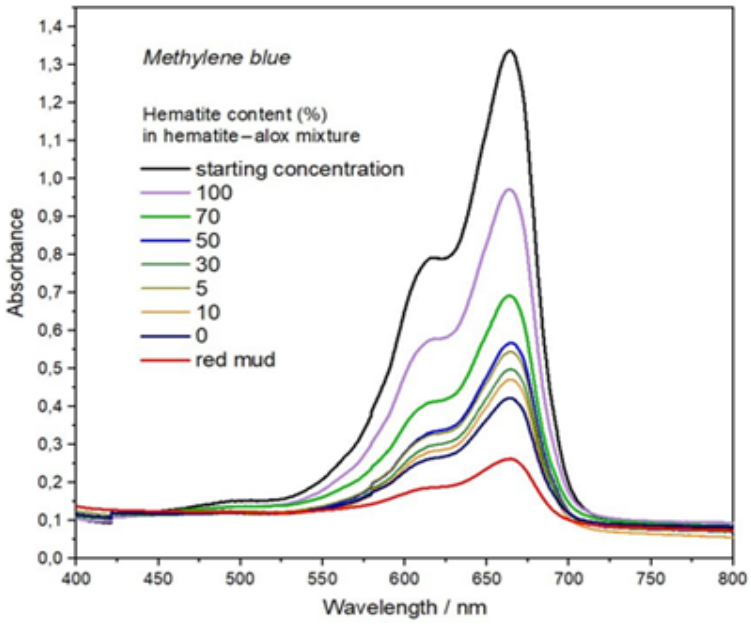

Figure 6: The degradation of model agent vs. hematite content. The starting concentration was 1.25 10-4mol/dm^3. UV-VIS absorption measurements.

Table 1: Influence of hematite content on the methylene blue concentration.

Hematite Content (%)	100	70	50	10	0	Pure red mud
Reduction of Concentration (%)	27.2±2	48.2±3	57.5±3	65.0±4	68.5±4	80.1±4

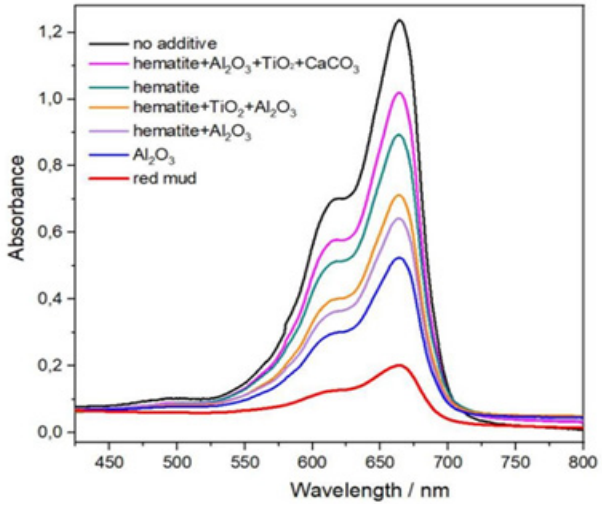

Figure 7: The degradation of model agent vs. various composition of red mud components. The starting concentration was 1.25 10-4mol/dm^3. UV-VIS absorption measurements.

The photodegradation effect of RM was compared with a new type of excellent adsorbent, chitosan (Figure 8). Red mud reveals more intensive reduction effect (94.0±5%) than chitosan (79±5%). After the model agent (MB) the photodegradation effect of RM was tested on potential real organic "waste" components; corticosterone and cortisone (Figure 9). Corticosterone is a 21-carbon steroid hormone of the corticosteroid type. Cortisone is a man-made version of a natural hormone cortisol. In the case of corticosterone, the reduction is lower; 45.0% in light and 21.6% in dark. Near 100% is the loss of cortisone amount in both cases in dark and in light conditions. On the basis of signal at 320nm, 81.9% was the decrease in concentration in light and 54.5% in dark. The ratio of photocatalytic effect and adsorption of RM on various materials are summarised in (Table 2) and calculated by means of "dark" and "light data". The data unambiguously reflect that the ratio of photocatalytic effect and adsorption strongly depends on the removed materials and both effects must be taken into account.

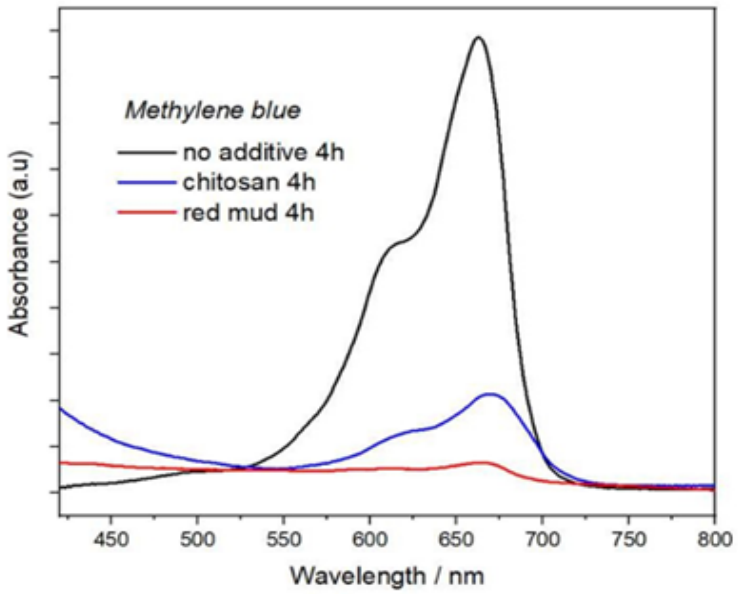

Figure 8: Comparison of the model agent's degradation by effect of red mud and chitosan. UV-VIS absorption measurements in $1.25 \cdot 10^{-4}$mol/dm^3 aqueous solution.

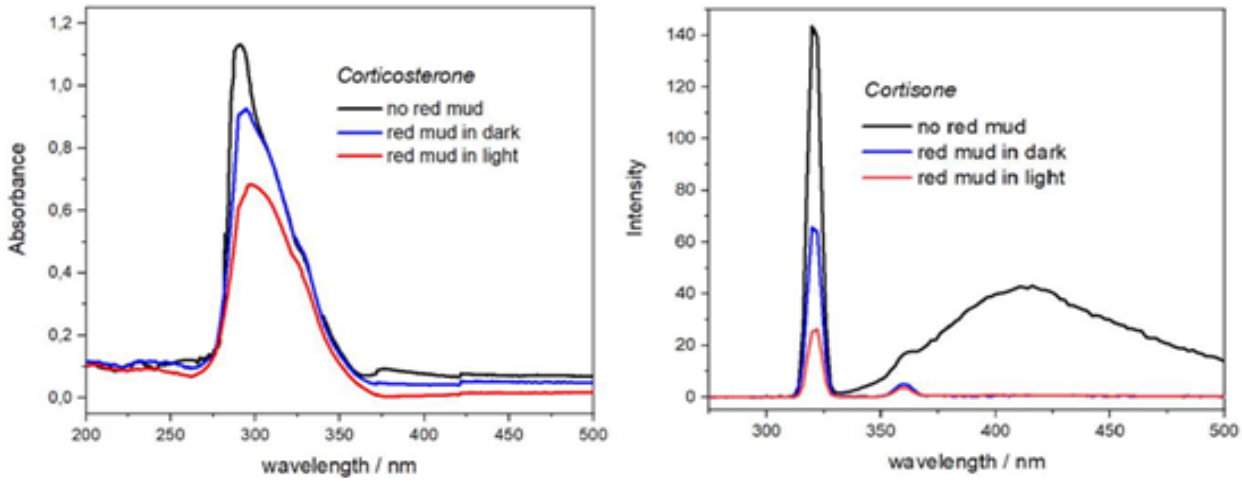

Figure 9: Comparison of photodegradation and adsorption effects of red mud on organic water pollution (steroid hormones) in visible light region from $7.5 \cdot 10^{-3}$mol/dm^3 (M) alcoholic solution. The concentration of cortisone was measured by fluorescence spectroscopy.

Table 2: Ratio of photocatalytic effect and adsorption of RM on various "waste" materials.

"Waste" Materials	Corticosterone	Cortisone	Methylene blue
Photocatalytic Effect	52%	33.50%	11%
Adsorption	48%	66.50%	89%

Conclusion

Red Mud (RM) is a by-product of alumina production, around 175 million tons of RM are generated (2021). The recycling rate of RM is only about 1-2% in other various technologies. The aim of this work was the utilisation of red mud as a functional material. Removal of the organic contaminants from wastewater as a functional application of RM has been chosen regarding the other very important environmentally friendly intention that is to clear the wastewaters. The photocatalytic properties of Red Mud (RM) were tested in the solution of analytical indicators used as model agents (methylene blue, Congo red, and crystal violet) and real organic pollutants (cortisone and corticosterone). In the case of model agents, the photodegradation effect was varied from 75% to 95% in the function of agent type, its concentration, and time of treatment. The test with potential organic contaminants resulted in 45 and close to 100% degradation in their concentration.

The photodegradation effect of RM was studied in the function of hematite. But increase of hematite ratio in the mixtures of hematite and aluminium oxide reduced the efficiency of mixtures. In order to achieve better chemical comparison to RM, the synthetic components of mixture were expanded. The measurements of photodegradation proved that Al_2O_3 is the most efficient compound of RM, after that hematite. Comparison of the concentration data of model agent reduced by "red mud" built up from synthetic components with original red mud it can be concluded that the smaller components of RM and their morphology have also important role in the photodegradation effect. The mechanism of the degradation effect of RM has been also clarified. The data obviously have proved both effects; photocatalysis and adsorption must be taken into account. The ratio of those strongly depends on the type of organic components. The very important economic result of this study is the removal of organic wastewater can be realised even in low concentration and using visible region for photodegradation instead of generally applied ultraviolet light.

References

1. Svobodova-Sedlackova A, Calderón A, Fernandez AI, Chimenos JM, Berlanga C, et al. (2024) Mapping the research landscape of bauxite by-products (red mud): An evolutionary perspective from 1995 to 2022. Heliyon 10(3): e24943.
2. Zeng H, Lyu F, Sun W, Zhang H, Wang L, et al. (2020) Progress on the industrial applications of red mud with a focus on China. Minerals 10(9): 773.
3. Landsberger S, Sharp A, Wang S, Pontikes Y, Tkaczyk AH (2017) Characterization of bauxite residue (red mud) for ^{235}U, ^{238}U, ^{232}Th and ^{40}K using neutron activation analysis and the radiation dose levels as modeled by MCNP. J Environmental Radioactivity 173: 97-101.
4. Khairul MA, Zanganeh J, Moghtaderi B (2018) The composition, recycling and utilisation of Bayer red mud. Resources, Conservation and Recycling 141: 483-498.
5. Olszewska JP, Meharg AA, Heal KV, Carey M, Gunn IDM, et al. (2016) Assessing the legacy of red mud pollution in a shallow freshwater lake: Arsenic accumulation and speciation in macrophytes. Environmental Science & Technology 50(17): 9044-9052.
6. Garau G, Silvetti M, Deiana S, Deiana P, Castaldi P (2011) Long-term influence of red mud on as mobility and soil physico-chemical and microbial parameters in a polluted sub-acidic soil. J Hazardous Materials 185(2-3): 1241-1248.
7. Kóth J, Sinkó K (2023) Geopolymer composites - In environmentally friendly aspects. Gels 9(3): 196.
8. Kaya K, Soyer-Uzun S (2016) Evolution of structural characteristics and compressive strength in red mud-metakaolin based geopolymer systems. Ceramics International 42(6): 7406-7413.
9. He J, Zhang G (2011) Geopolymerization of red mud and fly ash for civil infrastructure applications. Geotechnical Special Publications 1: 1287-1296.
10. Pontikes Y, Angelopoulos GN (2013) Bauxite residue in cement and cementitious applications: Current status and a possible way forward. Resources, Conservation and Recycling 73: 53-63.
11. Tian K, Wang Y, Dong B, Fang G, Xing F (2022) Engineering and micro- properties of alkali-activated slag pastes with Bayer red mud. Construction and Building Materials 351: 128869.
12. Ascensão G, Seabra MP, Aguiar JB, Labrincha JA (2017) Red mud-based geopolymers with tailored alkali diffusion properties and pH buffering ability. J Cleaner Production 148: 23-30.
13. Sahu MK, Mandal S, Dash SS, Badhai P, Patel RK (2013) Removal of Pb(II) from aqueous solution by acid activated red mud. J Environmental Chemical Engineering 1(4): 1315-1324.
14. Faria C, Vaz-Moreira I, Serapicos E, Nunes OC, Manaia CM (2009) Antibiotic resistance in coagulase-negative staphylococci isolated from wastewater and drinking water. Science of The Total Environment 407(12): 3876-3882.
15. Pleus RC, Snyder SA, Bruce GM (2010) Toxicological relevance of pharmaceuticals in drinking water. Environmental Science & Technology 44(14): 5619-5626.
16. Kondor AC, Jakab G, Vancsik A, Filep T, Szeberényi J, et al. (2020) Dataset of pharmaceuticals in the Danube and related drinking water wells in the Budapest region. Data in Brief 32: 106062.
17. Chauhan M, Saini VK, Suthar S (2020) Ti-pillared montmorillonite clay for adsorptive removal of amoxicillin, imipramine, diclofenac-sodium, and paracetamol from water. J Hazardous Materials 399: 122832.
18. Lebeau T, Lelièvre C, Buisson H, Cléret D, Van de Venter LW, et al. (1998) Immersed membrane filtration for the production of drinking water: combination with PAC for NOM and SOCs removal. Desalination 117(1-3): 219-231.
19. Changotra R, Rajput H, Dhir A (2019) Treatment of real pharmaceutical wastewater using combined approach of Fenton applications and aerobic biological treatment. J Photochemistry and Photobiology A: Chemistry 376: 175-184.
20. Hojamberdiev M, Czech B, Göktaş AC, Yubuta K, Kadirova ZC (2020) SnO_2@ZnS photocatalyst with enhanced photocatalytic activity for the degradation of selected pharmaceuticals and personal care products in model wastewater. J Alloys and Compounds 827: 154339.
21. de Andrade JR, Oliveira MF, da Silva MGC, Vieira MGA (2018) Adsorption of pharmaceuticals from water and wastewater using nonconventional low-cost materials: A review. Industrial & Engineering Chemistry Research 57(9): 3103-3127.
22. Cao Y, Nakhjiri AT, Ghadiri M (2021) Numerical investigation of ibuprofen removal from pharmaceutical wastewater using adsorption process. Scientific Reports 11: 24478.
23. Teixeira S, Gurke R, Eckert H, Kühn K, Fauler J, et al. (2016) Photocatalytic degradation of pharmaceuticals present in conventional treated wastewater by nanoparticle suspensions. J Environmental Chemical Engineering 4(1): 287-292.
24. Rioja N, Benguria P, Peñas FJ (2014) Competitive removal of pharmaceuticals from environmental waters by adsorption and photocatalytic degradation. Environmental Science and Pollution Research 21: 11168-11177.
25. Abdullah M, Iqbal J, Rehman MSU, Khalid U, Mateen F, et al. (2023) Removal of ceftriaxone sodium antibiotic from pharmaceutical

wastewater using an activated carbon-based TiO_2 composite: Adsorption and photocatalytic degradation evaluation. Chemosphere 317: 137834.

26. Ismael M (2020) Enhanced photocatalytic hydrogen production and degradation of organic pollutants from Fe(III) doped TiO_2 nanoparticles. J Environmental Chemical Engineering 8(2): 103676.
27. Asif AH, Wang S, Sun H (2021) Green chemistry perspectives in the treatment of industrial wastes using innovative photocatalytic methods. Current Opinion in Green and Sustainable Chemistry 28: 100447.
28. Lazar MA, Varghese S, Nair SS (2012) Photocatalytic water treatment by titanium dioxide: recent updates. Catalysts 2(4): 572-601.
29. Schneider J, Matsuoka M, Takeuchi M, Zhang J, Horiuchi Y, et al. (2014) Understanding TiO_2 photocatalysis: Mechanisms and materials. Chemical Reviews 114(19): 9919-9986.
30. Huerta-Fontela M, Galceran MT, Ventura F (2011) Occurrence and removal of pharmaceuticals and hormones through drinking water treatment. Water Research 45(3): 1432-1442.
31. Tolod KR, Hernández S, Quadrelli EA, Russo N (2019) Chapter 4 - Visible light-driven catalysts for water oxidation: Towards solar fuel biorefineries. Studies in Surface Science and Catalysis 178: 65-84.
32. Wheeler DA, Wang G, Ling Y, Li Y, Zhang JZ (2012) Nanostructured hematite: Synthesis, characterization, charge carrier dynamics, and photoelectrochemical properties. Energy & Environmental Science 5: 6682-6702.
33. Zhang X, Li H, Wang S, Fan FRF, Bard AJ (2014) Improvement of hematite as photocatalyst by doping with tantalum. J Physical Chemistry C 118(30): 16842-16850.
34. Chen YH, Lin CC (2014) Effect of nano-hematite morphology on photocatalytic activity. Physics and Chemistry of Minerals 41: 727-736.
35. Gonçalves NPF, Olhero SM, Labrincha JA, Novais RM (2023) 3D-printed red mud/metakaolin-based geopolymers as water pollutant sorbents of methylene blue. J Cleaner Production 383: 135315.
36. Tehubijuluw H, Subagyo R, Yulita MF, Nugraha RE, Kusumawati Y, et al. (2021) Utilization of red mud waste into mesoporous ZSM-5 for methylene blue adsorption-desorption studies. Environmental Science and Pollution Research 28(28): 37354-37370.
37. Hu H, Yang Y, Zhou G, Wang N, Gu H (2024) Hydrothermal chemical modification of red mud for efficient adsorption of methylene blue. Environmental Technology 16: 1-14.
38. Samal S (2021) Utilization of red mud as a source for metal ions - A review. Materials 14(9): 2211.
39. Atasoy A (2005) An investigation on characterization and thermal analysis of the Aughinish red mud. J Thermal Analysis and Calorimetry 81: 357-361.
40. Pascual-Cosp J, Corpas-Iglesias F, Beceiro JL, Benítez-Guerrero M, Artiaga R (2009) Thermal characterization of a Spanish red mud. J Thermal Analysis and Calorimetry 96: 407-412.